RAPID COMMUNICATION

Emergent reversible giant electroresistance in spacially confined $La_{0.325}Pr_{0.3}Ca_{0.375}MnO_3$ wires*

Cui Li-Min(崔丽敏), Li Jie(李 洁)†, Wang Jia(王 佳), Zhang Yu(张 玉), and Zheng Dong-Ning(郑东宁)‡

Beijing National Laboratory for Condensed Matter Physics, Institute of Physics, Chinese Academy of Sciences, Beijing 100190, *China*

(Received 20 May 2014; revised manuscript received 27 May 2014; published online 24 July 2014)

Micro-patterning is considered to be a promising way to analyze phase-separated manganites. We investigate resistance in micro-patterned $La_{0.325}Pr_{0.3}Ca_{0.375}MnO_3$ wires with width of 10 μm, which is comparable to the phase separation scale in this material. A reentrant of insulating state at the metal–insulator temperature T_p is observed and a giant resistance change of over 90% driven by electric field is achieved by suppression of this insulating state. This resistance change is mostly reversible. The *I*–*V* characteristics are measured in order to analyze the origin of the giant electroresistance and two possible explanations are proposed.

Keywords: metal–insulator transition, micro-wire, phase separation, manganites

PACS: 71.30.+h, 78.30.cd, 64.75.Gh **DOI:** 10.1088/1674-1056/23/9/097103

1. Introduction

Perovskite manganites have attracted much attention during the last two decades for their novel properties, such as colossal magnetoresistance (CMR), charge ordering,[1–3] and phase separation.[4,5] The interplay between charge, spin, and lattice in these compounds leads to a very rich phase diagram, which is usually highlighted by coexistence of ferromagnetic metallic (FMM) and charge-ordering insulating (COI) phases in a wide temperature region. This phase separation phenomenon is considered to be crucial for the electric and magnetic properties in these materials. For instance, the novel CMR is due to an enhanced FMM phase percolation through COI phase by applied magnetic field, and thus a giant decrease in resistance takes place. As reported in the literatures, phase-separated manganites were analyzed directly by magnetic force microscopy (MFM)[6–9] and scanning tunneling microscopy (STM),[10,11] which presented evolution of the phase separation state with temperature and applied electric and magnetic field. In most cases, the scale of phase separation is in nanometer scale.[10,12] However, micrometer-scale phase separation of FMM/COI phases was observed in some narrow-band systems.[6,8] For A-site doping by ions with smaller radius in ABO_3-type perovskite manganites, band width is reduced and coexistence of large domains is possible. This phenomenon has brought about intense interest in such materials, where it is possible to detect the behavior of isolated domains by confining the sample dimension to the phase separation scale. Novel features hidden by average effect may show up in these micro-structures. Using this method, a number of notable results have been reported.[13–18] Sharp jumps of resistance were observed in 1.6-μm-wide (La, Pr, Ca)MnO_3 (LPCMO) wire.[14] The *I*–*V* curve of (Pr, Sr, Ca)MnO_3 (PCSMO) wires with width of about 1 μm presented step-like nature.[15] The first-order metal–insulator transition (MIT) showed fluctuations in LPCMO wires with width of 10 μm.[17] All of these results point to percolative conductance introduced by single domain percolation. Reentrant of insulating state was observed at temperature lower than the typical metal–insulator transition in 10-μm wires of LPCMO and (La, Ba)MnO_3 (LBMO),[16,18] which is much different from that in bulk or films. The modulation of such reentrant insulating state was performed by applying magnetic field in these manganite wires,[16] which indicates that the micrometer-scale phase separation in these materials may play a crucial role.

In this work, we perform measurements on 10-μm-wide $La_{0.325}Pr_{0.3}Ca_{0.375}MnO_3$ wires fabricated from epitaxial films. A reentrant of insulating state is observed below the typical MIT temperature T_p. By applying electric field, the reentrant insulating state is suppressed and finally diminished. This electric field suppression of the insulating state leads to giant resistance decrease. By measuring *I*–*V* characteristics, two possible tunneling mechanisms are proposed relating to two types of conduction barriers. Resistance fluctuations in this reentrant insulating state are also analyzed at different voltages.

*Project supported by the National Basic Research Program of China (Grant Nos. 2011CBA00106 and 2014CB921401) and the National Natural Science Foundation of China (Grant Nos. 11174342, 91321208, and 11374344).

†Corresponding author. E-mail: lijie@iphy.ac.cn

‡Corresponding author. E-mail: dzheng@aphy.iphy.ac.cn

© 2014 Chinese Physical Society and IOP Publishing Ltd

2. Experimental details

$La_{0.325}Pr_{0.3}Ca_{0.375}MnO_3$ (LPCMO) thin films with thickness of 90 nm were deposited on (001)-$LaAlO_3$ (LAO) substrate by pulsed laser deposition (PLD). The deposition temperature was 800 °C, while the energy of laser pulses was 450 mJ with a repetition rate of 2 Hz. The films were deposited in oxygen atmosphere with a pressure of 60 Pa. After deposition, the films were annealed at 540 °C for about 40 min in 1 atmosphere oxygen. Film characterization by X-ray diffraction (XRD) is shown in Fig. 1(a), which shows well *c*-axis epitaxial growth with no detectable impurity phase. Wires with a dimension of 10 μm × 50 μm were fabricated on the thin films by ultraviolet lithography and argon-ion milling. Electrical leads were attached to electrodes by using conducting silver paste. Optical micro-photography of the device is shown in Fig. 1(b). There are two separated wires on one chip. Van der Pauw method and standard four-probe method were employed for electric transport characterization of the films and wires, respectively, with a probe constant current of 10 nA. Two-probe method was used for analysis of the resistance change driven by electric field and *I*–*V* characteristics.

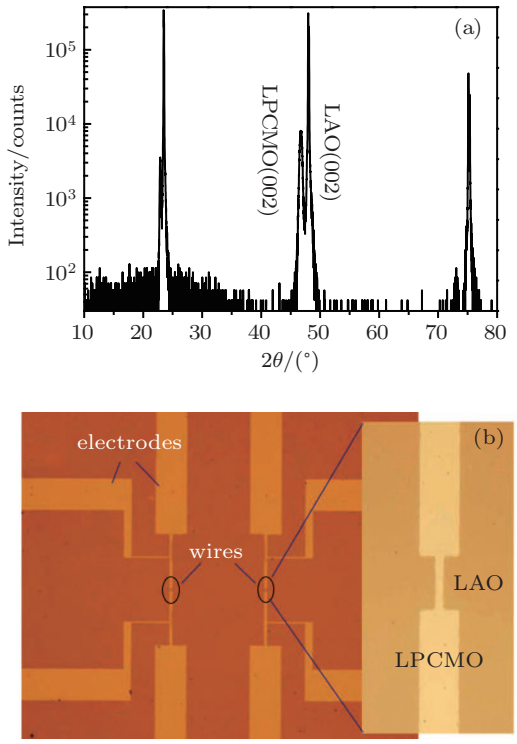


Fig. 1. (color online) (a) XRD pattern of the deposited film. (b) Optical photography of the patterned device.

3. Results and discussion

3.1. Reentrant insulating state in micro-wire

Resistance versus temperature curves were measured upon cooling before and after wire patterning. As shown in Fig. 2, the normalized resistance ($R/R_{290\,K}$) of the wires is very similar to that of the film above 110 K, indicating no obvious material degeneration during the micro-patterning process. However, a reentrance of insulating state shows up below 110 K and a re-emergent MIT happens with a sharp resistance jump at 91 K in one of the wires, while nothing is observed in the other one. We have prepared a number of samples and the reemergent MIT peak is only observed in some of them. Also, the resistance peak temperature T_p varies from one sample to another. This reentrant phenomenon appears, at first glance, to be surprise since it is only seen in some of the wire samples. However, we suggest that it may be understood by taking the phase separation into account. According to the phase separation picture, the LPCMO is strongly phase separated in a large temperature region. In the 10-μm wires, single FMM domain in this stage is too small to dominate the wire conductance, so resistance still shows a collective feature. No sharp resistance drop, as reported in confined LPCMO with narrower wire dimension of 0.6 μm and 1.6 μm,[14,19] would take place. As temperature decreases, the FMM domains enlarge to across several micrometers and dominate the conducting path[8] and the wire resistance drops quickly. At this stage, a residual COI domain or a boundary between FMM domains with different spin-polarized directions would act as conduction barriers and bring about a reentrance of insulating state in the wire. We believe that the variety of reentrant insulating state in different wires could be understood by considering the random spacial distribution of the phase-separated domains in the wire samples. Such a reentrant insulating state is also reported in other spatially confined manganites.[16,18] The wire resistance varies a lot with the measurement cycles in Ref. [18], which was attributed to random emerging of COI domains. However, in our wire samples, resistance is roughly reproducible with repeated measurement runs. It indicates a local memory effect of the conduction barriers, which may be related to crystalline defects as demonstrated in similar materials by MFM mapping.[7,9]

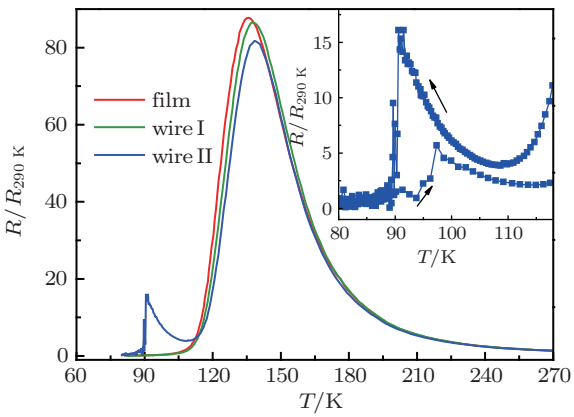


Fig. 2. (color online) Normalized resistance ($R/R_{290\,K}$) versus temperature of the film and the micro-patterned wires on the same chip. Inset: zoom-in on the reentrant insulating state with thermal hysteresis.

3.2. Giant resistance change driven by electric field

Electric field driven effect of this reentrant insulating state in wire II is analyzed by varying the probe voltage applied to the wire. This reemergent MIT is suppressed with increasing probe voltage and totally vanishes at a voltage of 30 V, as shown in Fig. 3(a), while the resistance of the typical MIT peak of manganites does not change much and even increases a little. This slight increase in resistance may be due to heat effect for the narrow conductance path in this stage. The giant electroresistance is over 90% at 93 K as the applied voltage varies from 0.2 V to 30 V. The resistance suppression is with small steps at relatively small voltages (1 V and 2 V). To characterize this electric field driven collapse of the reentrant insulating state, the I–V curve is measured at 100 K and the normalized dynamic conductance G/G_0, where dynamic conductance $G = \mathrm{d}I/\mathrm{d}V$ and G_0 is the dynamic conductance at zero bias, is calculated, as shown in Fig. 3(b). The I–V curve is nonlinear and mostly reversible with a small hysteresis at high voltages. The decrease in G/G_0 at voltages larger than 15 V may be due to thermal effect by current heating, which corresponds to the resistance hysteresis in the I–V curve at a relatively fast voltage sweeping rate of 0.3 V·s^{-1}.

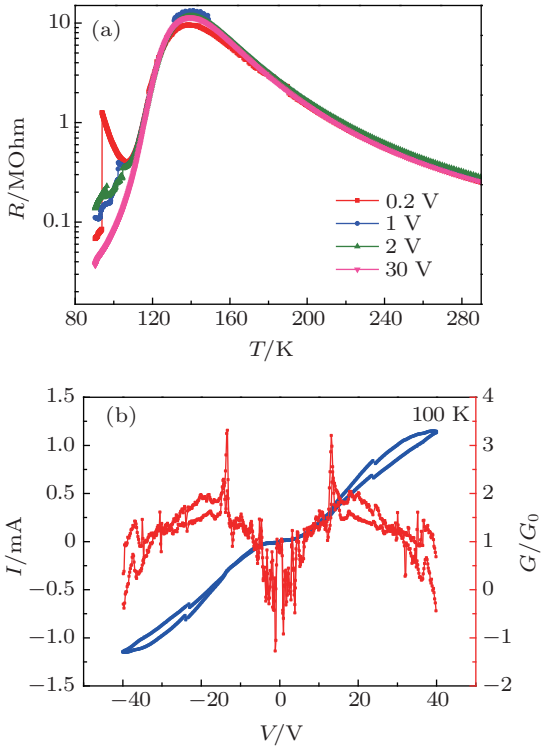


Fig. 3. (color online) (a) Resistance versus temperature at different voltages. (b) I–V characteristics (left axis) with calculated G/G_0 (right axis).

In another wire with the same dimension, the reentrant insulating state is much more significant than that in wire II, which indicates that a stronger conduction barrier exists in the wire. Similar voltage driving measurements and I–V characteristics were performed at 77 K. Results are shown in Fig. 4. It shows a very similar collapse of the reentrant insulating state with applied external electric field. The I–V curve is nonlinear and totally reversible, while G/G_0 appears to be very different from that in wire II.

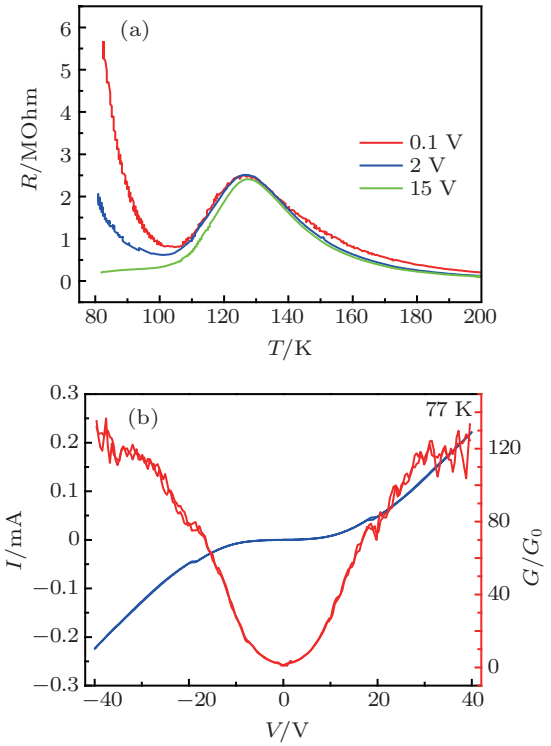


Fig. 4. (color online) (a) Resistance versus temperature at different voltages in another wire. (b) I–V characteristics (left axis) with calculated G/G_0 (right axis).

It was reported that electric field could induce insulating phase melting into metallic phase and cause significant resistance reduction,[20–22] in which a big hysteresis of the I–V curve is expected.[23] The approximate reversibility of the I–V curve in both wires indicates that the electric field induced collapse of the insulating state is dominated by tunneling through conduction barriers, but not the first-order phase transition. Two possible types of such conduction barriers are shown in Fig. 5. In strong phase separation region, a large COI domain may block the conduction path in the wire (Fig. 5(a)). As a result, the wire resistance shows insulating. In addition, there are domain walls between FMM domains with different spin-polarized directions.[24] When current flows through these domain walls, spin-flip scattering may contribute to the resistance increasing at lower temperatures (Fig. 5(b)). In our 10 μm × 50 μm wires, both kinds of barriers may contribute to the reentrance of insulating state. Tunneling through or collapse of these conduction barriers causes a significant drop of resistance observed here.

Figure 6 shows resistance at different voltages derived from the I–V curves mentioned above. In wire II, resistance at 100 K shows fluctuations at voltages under 5 V, and then decreases rapidly as voltage increases gradually. At voltages

larger than 15 V, reduction of resistance slows down as voltage further increases. Inset of Fig. 6 shows resistance fluctuations with time at different voltages, which presents more details of this tunneling process. Below 5 V, resistance shows fluctuation feature and seems to prefer the higher values of about 170 kΩ for 2 V, while a larger voltage (3 V) favors the lower value of about 150 kΩ. As voltage increases further (6, 8, and 30 V), resistance is stable with time. This resistance fluctuation with relatively weak electric field may be sign of random formation of tunneling paths.

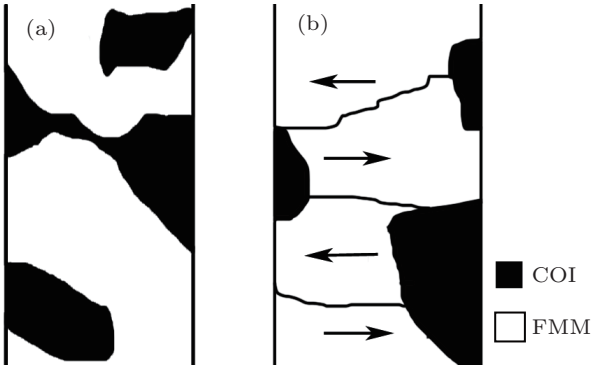


Fig. 5. Schematic diagram of conduction barriers of (a) residual COI domain and (b) domain walls between FMM domains with different spin-polarized directions.

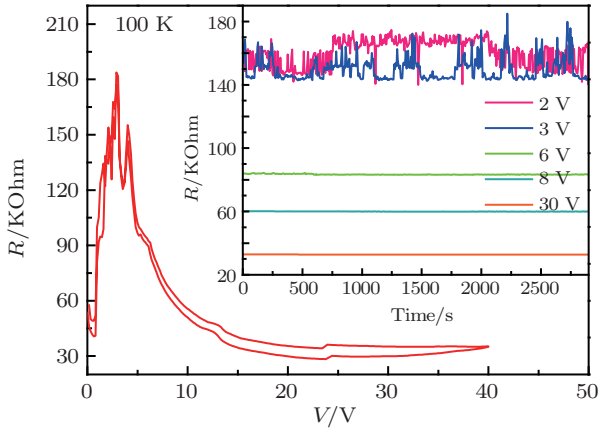


Fig. 6. (color online) Resistance as a function of voltage in wire II at 100 K. Inset: resistance fluctuations at different voltages.

4. Conclusions

In this work, we report reentrant insulating state in micro-patterned LPCMO wires. A giant electroresistance of more than 90% was observed by electric field suppression of this reentrant insulating state. The resistance change is mostly reversible. By measuring *I*–*V* characteristics, the conductance shows tunneling feature with conduction barriers of COI domains or boundaries between FMM domains with different spin-polarized directions. Resistance at this reentrant insulating region shows fluctuations at low voltages. This indicates the random formation of tunneling path, which becomes stable at high voltages.

References

[1] Prellier W, Lecoeur P and Mercey B 2001 *J. Phys.: Condens. Matter* **13** R915
[2] Jin S, Tiefel T H, McCormack M, Fastnacht R, Ramesh R and Chen L 1994 *Science* **264** 413
[3] Siwach P K, Singh H K and Srivastava O N 2008 *J. Phys.: Condens. Matter* **20** 273201
[4] Moreo A 1999 *Science* **283** 2034
[5] Dagotto E, Hotta T and Moreo A 2001 *Phys. Rep.* **344** 1
[6] Uehara M, Mori S, Chen C and Cheong S W 1999 *Nature* **399** 560
[7] Sarma D, Topwal D, Manju U, Krishnakumar S, Bertolo M, La Rosa S, Cautero G, Koo T, Sharma P, Cheong S W and Fujimori A 2004 *Phys. Rev. Lett.* **93** 097202
[8] Zhang L, Israel C, Biswas A, Greene R L and de Lozanne A 2002 *Science* **298** 805
[9] Wu W, Israel C, Hur N, Park S, Cheong S W and de Lozanne A 2006 *Nat. Mater.* **5** 881
[10] Rößler S, Ernst S, Padmanabhan B, Elizabeth S, Bhat H, Steglich F and Wirth S 2008 *Europhys. Lett.* **83** 17009
[11] Fäth M, Freisem S, Menovsky A, Tomioka Y, Aarts J and Mydosh J 1999 *Science* **285** 1540
[12] Dagotto E 2005 *Science* **309** 257
[13] Wei J and Natelson D 2011 *Nanoscale* **3** 3509
[14] Zhai H Y, Ma J, Gillaspie D, Zhang X, Ward T, Plummer E and Shen J 2006 *Phys. Rev. Lett.* **97** 167201
[15] Wu T and Mitchell J 2006 *Phys. Rev. B* **74** 214423
[16] Ward T, Liang S, Fuchigami K, Yin L, Dagotto E, Plummer E and Shen J 2008 *Phys. Rev. Lett.* **100** 247204
[17] Ward T Z, Gai Z, Guo H W, Yin L F and Shen J 2011 *Phys. Rev. B* **83** 125125
[18] Nakajima T, Tsuchiya T, Ueda Y and Kumagai T 2009 *Phys. Rev. B* **80** 020401
[19] Singh-Bhalla G, Selcuk S, Dhakal T, Biswas A and Hebard A 2009 *Phys. Rev. Lett.* **102** 077205
[20] Garbarino G, Acha C, Levy P, Koo T and Cheong S 2006 *Phys. Rev. B* **74** 100401
[21] Asamitsu A, Tomioka Y, Kuwahara H and Tokura Y 1997 *Nature* **388** 50
[22] Yi H, Choi T and Cheong S W 2009 *Appl. Phys. Lett.* **95** 063509
[23] Yi H T, Choi T and Cheong S W 2009 *Appl. Phys. Lett.* **95** 063509
[24] He J, Volkov V, Beleggia M, Asaka T, Tao J, Schofield M and Zhu Y 2010 *Phys. Rev. B* **81** 094427